

## ORIGINAL ARTICLE

# In vitro and in vivo drug disposition of cilengitide in animals and human

Hugues Dolgos, Achim Freisleben, Elmar Wimmer, Holger Scheible, Friedrich Krätzer, Tetsuo Yamagata, Dieter Galleman & Markus Fluck

Global Early Development/Quantitative Pharmacology and Drug Disposition (QPD), Merck, Grafing, Germany

## Keywords

Animals and human, cilengitide, hepatobiliary, in vitro and in vivo, pharmacokinetics, sandwich-cultured hepatocytes

## Correspondence

Hugues Dolgos, Global Early Development/Quantitative Pharmacology and Drug Disposition (QPD), Merck KGaA, Frankfurter Strasse 250, 64293, Darmstadt, Germany.  
Tel: +49(0)6151 72 4818;  
Fax: +49(0)6151 72 91 5993;  
E-mail: hugues.dolgos@merckgroup.com

## Funding Information

The work was supported by Merck.

Received: 25 August 2015; Revised: 11 December 2015; Accepted: 30 December 2015

*Pharma Res Per*, 4(2), 2016, e00217,  
doi:10.1002/prp2.217

doi: 10.1002/prp2.217

## Abstract

Cilengitide is very low permeable (1.0 nm/sec) stable cyclic pentapeptide containing an Arg-Gly-Asp motif responsible for selective binding to  $\alpha v\beta 3$  and  $\alpha v\beta 5$  integrins administered intravenously (i.v.). In vivo studies in the mouse and Cynomolgus monkeys showed the major component in plasma was unchanged drug (>85%). These results, together with the absence of metabolism in vitro and in animals, indicate minimal metabolism in both species. The excretion of [ $^{14}\text{C}$ ]-cilengitide showed profound species differences, with a high renal excretion of the parent drug observed in Cynomolgus monkey (50% dose), but not in mouse (7 and 28%: m/f). Consistently fecal (biliary) secretion was high in mouse (87 and 66% dose: m/f) but low in Cynomolgus monkey (36.5%). Human volunteers administered with [ $^{14}\text{C}$ ]-cilengitide showed that most of the dose was recovered in urine as unchanged drug (77.5%, referred to Becker et al. 2015), indicating that the Cynomolgus monkey was the closer species to human. In order to better understand the species difference between human and mouse, the hepatobiliary disposition of [ $^{14}\text{C}$ ]-cilengitide was determined in sandwich-cultured hepatocytes. Cilengitide exhibited modest biliary efflux (30–40%) in mouse, while in human hepatocytes this was negligible. Furthermore, it was confirmed that the uptake of cilengitide into human hepatocytes was minor and appeared to be passive. In summary, the extent of renal and biliary secretion of cilengitide appears to be highly species specific and is qualitatively well explained using sandwich hepatocyte culture models.

## Abbreviations

ADME, absorption, distribution, metabolism, and excretion; AUC, area under the curve; BDDCS, biopharmaceutical drug disposition classification system; CL, plasma clearance; HPLC, high-performance liquid chromatography; hbf, hepatic blood flow; i.v., intravenous; LC/MS/MS, liquid chromatography/mass spectrometry/mass spectrometry; LSC, liquid scintillation counting; Po/w, octanol–water partition coefficient; P450, cytochrome P450.; Vdss, volume of distribution at steady state.

## Introduction

Cilengitide (EMD121974; MSC1097999C; see Figure 1) is a homodetic, head-to-tail cyclized Arg-Gly-Asp (RGD)-containing pentapeptide with the chemical structure cyclo-(Asp-D-Phe-N-MeVal-Arg-Gly). The physicochemical

properties of the drug include molecular formula  $\text{C}_{27}\text{H}_{40}\text{N}_8\text{O}_7$ , molecular mass of 588.67 g/mol, partition coefficient Po/w of 0.0096 ( $\log \text{Po/w} = -2.0$ ), and hygroscopic.

Cilengitide is a potent and selective antagonist of the  $\alpha v\beta 3$  and  $\alpha v\beta 5$  integrin receptors, that are involved in

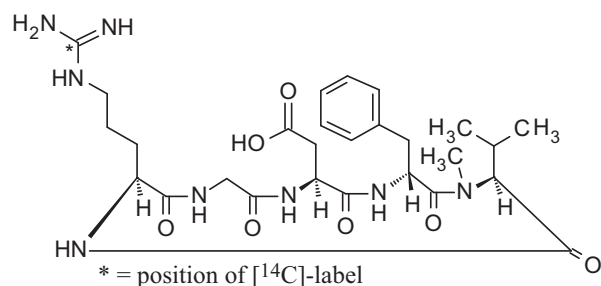


**Figure 1.** Structure of [<sup>14</sup>C]-cilengitide.

tumor cell growth and the formation of new tumor-related blood vessels (angiogenesis) in the tumor microenvironment and are overexpressed or aberrantly expressed in many cancers (Aoudjit and Vuori 2001; Courter *et al.* 2005; Dolfi *et al.* 1998; Mas-Moruno *et al.* 2010; Miyamoto *et al.* 1996; Moehler *et al.* 2001). By blocking integrins, tumor angiogenesis is prevented, providing the prospect of broader spectra of indications for cilengitide (e.g., glioblastoma, advanced solid tumors, pancreatic, prostate, non-small cell lung, and head and neck cancer). Experimental studies have shown that cilengitide demonstrates antiangiogenic, direct antitumor and antimigratory properties, and can suppress angiogenesis and tumor growth in vitro and in vivo (Dechantsreiter *et al.* 1999; MacDonald *et al.* 1999, 2001; Maurer *et al.* 2009; Mitjans *et al.* 2000; Raguse *et al.* 2004; Yamada *et al.* 2006). Cilengitide acts both as a monotherapy and as an enhancer of coadministered therapies, and affects cell proliferation of both tumor and vascular compartments.

Clinical studies with cilengitide have demonstrated antitumor effects in cancer patients, and the drug appears to enhance the efficacy of certain cytotoxic and targeted anticancer interventions (Albert *et al.* 2006; Bradley *et al.* 2011; Friess *et al.* 2006; Gilbert *et al.* 2011; Kurozumi *et al.* 2012; Stupp *et al.* 2010; Tentori *et al.* 2008). Although unique in its mode of action, cilengitide did not meet its primary endpoint of significantly increasing overall survival when added to the current standard chemoradiotherapy regimen (i.e., temozolomide and radiotherapy) for treatment of cancer patients with newly diagnosed glioblastoma (a very aggressive type of brain tumor) in the most advanced phase III clinical trial (Soffietti *et al.* 2014).

This paper summarizes the in vitro and in vivo drug disposition and metabolism studies elucidating the mechanisms of cilengitide's pharmacokinetic disposition in animals and humans. Profound interspecies difference in the disposition of the drug have been seen, however, no such differences were observed in the classical in vitro metabolism studies. Therefore, additional in vitro experiments were performed to elucidate these pharmacokinetic

differences and – together with data from the human mass balance trial – clarify how cilengitide is eliminated in human.

## Materials and Methods

Cilengitide (chemical name: Cyclo-(Asp-D-Phe-N-MeVal-Arg-Gly) and [<sup>14</sup>C]-guanidine cilengitide, with chemical and radiochemical purities of >98% by high-performance liquid chromatography (HPLC), were synthesized by Merck (Grafing, Germany) (Fig. 1). The internal standard used for liquid chromatography/mass spectrometry/mass spectrometry (LC/MS/MS) bioanalysis of cilengitide in mouse and Cynomolgus monkey plasma was EMD66203 [chemical name: Cyclo-(Arg-Gly-Asp-DPhe-Val)]. Its chemical purity was >98% by HPLC and it has been synthesized by Merck.

## In vivo studies with cilengitide in mouse and monkey

The pharmacokinetics, distribution, metabolism, and excretion of [<sup>14</sup>C]-cilengitide (2.5 mg/kg; 4.2 μmol/kg) were investigated in male and female mice (NMRI) following intravenous (i.v.) bolus administration. The radioactive dose received by each mouse was approximately 2 mol/L Bq/kg. The biological stability of the radiolabel was shown to be acceptable, with less than 0.1% of the dose being exhaled by rats as [<sup>14</sup>C]-CO<sub>2</sub> within 72 h after dosing.

Animal studies have been approved by the appropriate animal welfare authority (Regierung von Oberbayern, Germany) and were conducted in compliance with European and federal guidelines for the use and care of laboratory animals.

## Plasma pharmacokinetics

Blood samples of mice were taken by exsanguinations ( $N = 3$ /time point) under anesthesia. Plasma was generated by centrifugation. Total [<sup>14</sup>C]-radioactivity was determined in plasma samples at predose, 0.1, 0.25, 0.5, 1.0, 2, 4, 8, 24, 48, and 72 h after dosing and analyzed for total radioactivity by liquid scintillation counting (LSC) on a TriCarb 460 D or TriCarb 4640 counter (PerkinElmer Inc., Waltham, MA). For total radioactivity analysis, blood samples ( $n = 3$ /time-point) were centrifuged (2 min at 10,000g) and 0.1–0.2 mL of the supernatant plasma was mixed with 5 mL Omni-Szintisol (MERCK) for LSC.

Plasma samples obtained from studies using unlabeled cilengitide were taken at predose, 0.1, 0.25, 0.5, 1.0, 2, 4, and 8 h after dosing and analyzed for parent compound by a validated LC/MS/MS assay (Table 1).

**Table 1.** LC/MS/MS conditions for cilengitide analysis.

LC-MS system	Perkin Elmer SCIEX mass spectrometer API-IIIplus Perkin Elmer binary LC pump 250 Perkin Elmer autosampler ISS-100
Mobile phase (isocratic)	acetonitrile/ammonium acetate buffer (0.01 mol/L, pH 4.3) (80/20, v/v)
Flow	0.3 mL/min
Injection volume	10 $\mu$ L
HPLC column	Waters C18 Symmetry, 15*2.1 mm, 5 $\mu$ m
MS mode	Turbo ion spray, positive
Ions detected for quantification	For cilengitide: m/z 589 $\rightarrow$ m/z 312 For IS: m/z 575 $\rightarrow$ m/z 459
Calibration range	5.00–1000 ng/mL
LLOQ	5.00 ng/mL (using 0.2 mL plasma)
Accuracy	97.3% to 113% for all QC levels
Precision	$\leq$ 5.17% for all QC levels

HPLC, high-performance liquid chromatography.

Pharmacokinetic parameters were determined using noncompartmental analysis

## Distribution

### Quantitative tissue distribution (dissection method)

Following i.v. dosing of [ $^{14}$ C]-cilengitide (2.5 mg/kg) to male and female mice ( $n = 3$ /time), the distribution of radioactivity to organs and tissues was determined at 0.1, 0.5, 2, 8, and 24 h after dosing. Larger organs like liver and brain were homogenized prior to combustion while small tissues like adrenals and eyes were combusted directly. Also carcasses were analyzed for remaining radioactivity. All samples were dried at about 60°C for 12 h before oxidized in a TriCarb 306 sample oxidizer and measured in liquid scintillation spectrometers Tri-Carb 460 D and/or TriCarb 4640 (PerkinElmer Inc.).

### Qualitative whole-body autoradiography

The distribution of radioactivity to organs and tissues was determined in male NMRI mice by qualitative whole-body autoradiography (WBA). At each time, one animal was killed with CO<sub>2</sub> at 0.1, 0.5, 1, 4, 8, and 24 h after dosing. The carcasses were frozen in a mixture of isopropanol and dry ice, and embedded in a wall paper glue preparation. Sections (25  $\mu$ mol/L) were produced using a cryomicrotome, dehydrated and then exposed to imaging plates 24–48 h in a shielding box. A Bioimaging analyzer (BAS 2000, Fujifilm Corporation, Tokyo, Japan) was used for read out of the imaging plates. Images are given in false color.

## Metabolite profiling

For metabolite profiling, aliquots of plasma taken at 0.1 and 0.25 h postdose were extracted twice with ethanol. Following centrifugation, the supernatants were combined and evaporated to dryness. The residue was dissolved in 200  $\mu$ L mobile phase (containing 250  $\mu$ g unlabeled cilengitide) and aliquots measured for radioactivity by LSC and by radio-HPLC for metabolites. The precipitates were washed three times with ethanol and the remaining radioactivity determined by LSC as [ $^{14}$ C]-CO<sub>2</sub> after combustion in a TriCarb 306 sample oxidizer (PerkinElmer Inc.). Aliquots (50 and 500  $\mu$ L) of urine samples taken at 0–8 and 8–24 h intervals were evaporated to dryness and the resultant residues reconstituted in 150  $\mu$ L mobile phase and analyzed by radio-HPLC for metabolites (Table 2). Fecal samples (0–8 and 8–24 h) were homogenized in water and aliquots (up to 1 g) extracted twice with ethanol. Due to the low amount of radioactivity that was extractable from feces, the precipitates were treated in an ultrasonic bath at 40°C/2 h with ethanol and the resultant extract analyzed by radio-HPLC for metabolites (Table 2). The amount of radioactivity remaining in the fecal precipitate after extraction was determined as [ $^{14}$ C]-CO<sub>2</sub> after combustion as described above.

The radioactive constituents in plasma, and excreta were separated using radio-HPLC method as outlined in Table 2. Detection was either by a radioactivity detector or by collecting the column effluent in 0.5 mL fractions and analyzed by LSC. Appropriate amounts of cilengitide (about 12.5  $\mu$ g/injection) were added as a reference to the samples before HPLC separation and detected by UV.

**Table 2.** HPLC (high-performance liquid chromatography) conditions for metabolic profiling in vivo mouse and monkey studies.

HPLC (high-performance liquid chromatography) system	Merck Hitachi HPLC pump L-6200/L-6200A Merck Hitachi autosampler AS-2000A with manual Rheodyne injection valve 7125
Radiodetector	Merck Hitachi UV detector L-4000/UV monitor 655A Berthold radioactivity monitor LB 506 C-1 with glass scintillator cell YG 400/YG 150 or Packard radioactivity monitor 525 TR LSC with liquid 500 $\mu$ L cell
Mobile phase (isocratic)	acetonitrile/ammonium acetate buffer (0.05 mol/L, pH 4) (19/80, v/v)
Flow	1 mL/min
Injection volume	100–150 $\mu$ L
HPLC column	Merck LiChroCart LiChrospher 100, RP8e, 150*4 mm, 5 $\mu$ m
UV detection at	230 nm
Total recovery of $^{14}$ C radioactivity	>95%

### Total radioactivity determination in excreta

Urine and feces were collected at 0–8, 8–24 h and then in 24 h-intervals up to 120 h after dosing. An aliquot (0.2 mL) of urine from each timed pooled sample ( $n = 3$ ) was analyzed for radioactivity by LSC. Fecal samples were homogenized in water and a small amount of stabilizer (carboxymethylcellulose, MERCK) added. Aliquots of 1 g were dried at 60°C/12 h and combusted in a sample oxidizer for radioactivity determination. At the end of the study, carcasses were minced and 0.5 g aliquots, combusted and analyzed for radioactivity. The tail of each animal was removed, cut into small segments and processed as detailed in tissue excision study for any residual radioactivity remaining at the injection site. All radioactive samples were measured by LSC using TriCarb 460 D and/or TriCarb 4640 counter (PerkinElmer Inc.).

### Monkey

The pharmacokinetics, metabolism, and excretion of [ $^{14}\text{C}$ ]-cilengitide (2.0 mg/kg; 3.4  $\mu\text{mol/kg}$ ) were studied in female *Cynomolgus* monkeys (*Macaca fascicularis*,  $n = 3$ ) after single i.v. bolus injection. The radioactive dose administered was approximately 1 mol/L Bq/kg.

### Plasma pharmacokinetics

Following administration of [ $^{14}\text{C}$ ]-cilengitide to female *Cynomolgus* monkeys, samples of plasma (1–2 mL) were taken at predose, 0.1, 0.5, 1.0, 2, 4, 8, 24, and 48 h after dosing. Samples were analyzed for total radioactivity by LSC and for parent compound by LC/MS/MS (Table 1). Sample extraction, analytical methodology, and calculation of pharmacokinetic (PK) parameters were similar to those used for the in vivo mouse study detailed above.

### Metabolite profiling

Aliquots of plasma (200–500  $\mu\text{L}$ ) taken at 0.1, 0.5, 1.0, 2, 4, and 8 h postdose, were extracted twice with ethanol (2 mL), centrifuged and aliquots (20 or 100  $\mu\text{L}$ ) measured for radioactivity by LSC and for metabolites by radio-HPLC (Table 2). The precipitates were assayed for total radioactivity by LSC following combustion in the sample oxidizer. Aliquots of urine (50 and 500  $\mu\text{L}$ ) from 0 to 8 h and 8 to 24 h collections and from the 24 h-intervals up to 120 h postdose were evaporated, reconstituted in 150  $\mu\text{L}$  mobile phase and analyzed by radio-HPLC for metabolites. Fecal samples were taken at the same intervals as urine were processed and analyzed using similar methods described above for the in vivo mouse study.

### Total radioactivity determination in excreta

Urine and feces were collected during 0–8 h, 8–24 h, and then in 24 h-intervals up to 120 h and analyzed by LSC for radioactivity as for the in vivo mouse study detailed above.

### In vivo studies in rat and rabbit

Besides mouse and monkey, the species employed in general toxicity assessment, rat and rabbit, were also investigated as preclinical species for reprotoxicity testing. Plasma pharmacokinetics was assessed either in preparatory PK-studies (rat) or from regulatory toxicity studies (rabbit). In Wistar rats, PK-samples were collected after an intravenous bolus injection at 0.1, 0.25, 0.5, 1, 2, 4, and 6 h postadministration. Plasma PK in Chinchilla rabbits were recorded after intravenous infusion (into the ear vein) at various dose levels (i.e., 50, 150, or 450 mg/kg/d; 85, 255, or 764  $\mu\text{mol/kg/d}$ ) with the following sampling times: before, and 2, 4, 4.25, 4.5, 5, 7, and 10 h after start of infusion (4 h). The test item was administered dissolved in phosphate buffer saline (pH 7.4) and plasma concentrations were analyzed applying LC/MS/MS.

Animal studies have been approved by the appropriate animal welfare authority (Regierung von Oberbayern, Munich, Germany) and were conducted in compliance with European and federal guidelines for the use and care of laboratory animals.

### Allometry scaling and dose predictions in human

Allometric scaling is a basic interspecies scaling method that employs in vivo pharmacokinetic parameters to extrapolate from animal models to human. As metabolism of cilengitide was shown to be minimal across species and the mode of administration is i.v., simple allometric scaling based on log body weight was considered sufficient and applied using the following equation:

$$\text{Log } Y = \log a + \text{blog } W$$

$Y$  = pharmacokinetic parameter (CL,  $V_{\text{dss}}$ );  $a$  = allometric coefficient;  $b$  = allometric exponent;  $W$  = body weight.

Half-life values were estimated based upon the predicted primary parameters of clearance (CL) and volume of distribution at steady state ( $V_{\text{dss}}$ ).

### In vitro incubations with cilengitide

#### Evaluation of hepatobiliary disposition

[ $^{14}\text{C}$ ]-cilengitide (10 and 250  $\mu\text{mol/L}$ ) was incubated in sandwich-cultured mouse (NMRI) and human hepato-

cytes ( $n = 3$ ) for 3 and 6 days, respectively, using a proprietary in vitro method (B-CLEAR<sup>®</sup> technology; Qualyst Transporter Solutions, LLC). This method enabled characterization of hepatic uptake, excretion, biliary clearance, intracellular concentration, and hepatic drug transporter interactions of the drug and its metabolites (Ghibellini et al. 2004, 2006, 2007). A positive system control of [<sup>3</sup>H]-taurocholate (1  $\mu$ mol/L, 10 min incubation) was performed to confirm transporter function. [<sup>14</sup>C]-cilengitide and [<sup>3</sup>H]-taurocholate were measured by LSC and as an additional control, a cytotoxicity test using lactate dehydrogenase (LDH) as a marker was performed. There were no consistent changes in the amounts of LDH found in the cell culture medium following exposure towards 250  $\mu$ mol/L cilengitide for up to 24 h, indicating that cilengitide does not cause cell toxicity (data not shown). Data were analyzed to yield intracellular concentrations ( $C_{ic}$ ), biliary clearance ( $CL_{bil}$ ), and biliary excretion index (BEI) using equations (1)–(3). The cellular volume of hepatocytes ( $V_{cell}$ ) was used as 8.06  $\mu$ L/mg protein. Accumulation<sub>Minus (-) Buffer</sub> (pmol/mg protein) represents the total mass of analyte inside the hepatocytes at the end of the incubation time period. Accumulation<sub>Plus (+) Buffer</sub> (pmol/mg protein) represents the total mass of compound taken up and excreted (cells + bile). The cellular accumulation parameters were corrected for non-specific binding.

$$C_{ic}(\mu M) = \frac{\text{Accumulation}_{\text{Minus}(-)\text{Buffer}}}{V_{cell}} \quad (1)$$

$$CL_{bil}(\text{mL}/\text{min}/\text{kg}) = \frac{\text{Accumulation}_{\text{Plus}(+)\text{Buffer}} - \text{Accumulation}_{\text{Minus}(-)\text{Buffer}}}{\text{AUC (i.e. Time} \cdot \text{Concentration}_{\text{Media}})} \quad (2)$$

$$\text{BEI}(\%) = \frac{\text{Accumulation}_{\text{Plus}(+)\text{Buffer}} - \text{Accumulation}_{\text{Minus}(-)\text{Buffer}}}{\text{Accumulation}_{\text{Plus}(+)\text{Buffer}}} \times 100 \quad (3)$$

In the supernatant and the cell lysate of human hepatocytes following incubation for 6 and 24 h with [<sup>14</sup>C]-cilengitide (250  $\mu$ mol/L), no indication for biotransformation of cilengitide was found by HPLC analysis (data not shown).

To demonstrate the suitability of the human B-CLEAR<sup>®</sup> cultures for metabolic profile characterization of cilengitide, the metabolic activity of three CYP enzymes, CYP1A2 (phenacetin, 100  $\mu$ mol/L), CYP2C19 (S-mephenytoin), and CYP3A4/5 (testosterone, 250  $\mu$ mol/L), was investigated during 30 min incubation. All batches of sandwich cultured human hepatocytes used in this study showed acceptable metabolic rate of the investigated CYP enzymes (data not shown).

## Uptake into hepatocytes

The uptake of cilengitide was determined in human suspension hepatocytes by incubating with drug at concentrations of 10  $\mu$ mol/L, 250  $\mu$ mol/L, and 10 mmol/L. The uptake was studied by separating the cells from incubation buffer using the oil-layer method and monitoring the time-dependent drug concentration in both compartments. Incubation times from 1 to 30 or 90 min were tested. The amount of test item was quantified by LC/MS/MS (Table 1). Transporter activity of the cryopreserved hepatocytes (Invitrogen, Corporation, part of Life Technologies, Carlsbad, CA, US) had been verified by the supplier by assessing the functionality of several uptake and efflux transporters (NTCP, BSEP, OATP1B1/3, MDR1, MRP2, and OCT1). Positive control substrates [<sup>3</sup>H]-[N-methyl-3H]-4-phenyl pyridinium acetate ([<sup>3</sup>H]-MPP<sup>+</sup>; ARC Inc., US) and [<sup>3</sup>H]-estradiol-17 $\beta$ -D-glucuronide ([<sup>3</sup>H]-E17 $\beta$ G, ARC Inc., St. Louis, MO, US) were tested in the study and clearly accumulated in hepatocytes after 3 min of incubation (data not shown), confirming the validity of the test system to investigate active uptake processes mediated by OATP1B1/1B3 and OCT1. An inhibitor cocktail consisting of 20  $\mu$ mol/L-rifampicin (inhibits P-gp, MRP1, OATP1A2, OATP1B1, OATP1B3 transporters), 20  $\mu$ mol/L-cyclosporine A (inhibits ASBT, BCRP, BSEP, P-gp, MRP1, MRP2, NTCP, OATP1B1, OATP1B3, OATP2B1), and 100  $\mu$ mol/L-quinidine (inhibits P-gp, MRP2, OAT3, OATP1A2, OCT1, OCT2, OCT3, OCTN1, OCTN2) was used for nonspecific transporter inhibition (all compounds purchased at Sigma-Aldrich Corporation, LLC., St Louis, MO, US).

## Results

### In vivo studies with cilengitide

#### Mouse

##### Pharmacokinetics

Mean plasma concentrations of radioactivity at 0.1 h after i.v. dose administration were 1340 and 2840 ng eq/mL in males and females, respectively. Concentrations then declined rapidly such that by 8 h postdose those were below the limit of detection (Fig. 2) resulting in very short elimination half-life ( $t_{1/2}$ ) values of 0.39 and 0.31 h. The (area under the curve, AUC) AUC<sub>0- $\infty$</sub>  value for radioactivity in females was approximately twice that observed in males (905 vs. 469 ng eq./mL/h).

At 0.1 h after i.v. dosing, mean plasma concentrations of cilengitide, that is, unchanged drug, were 1240 and 2493 ng/mL in males and females, respectively. Concentra-

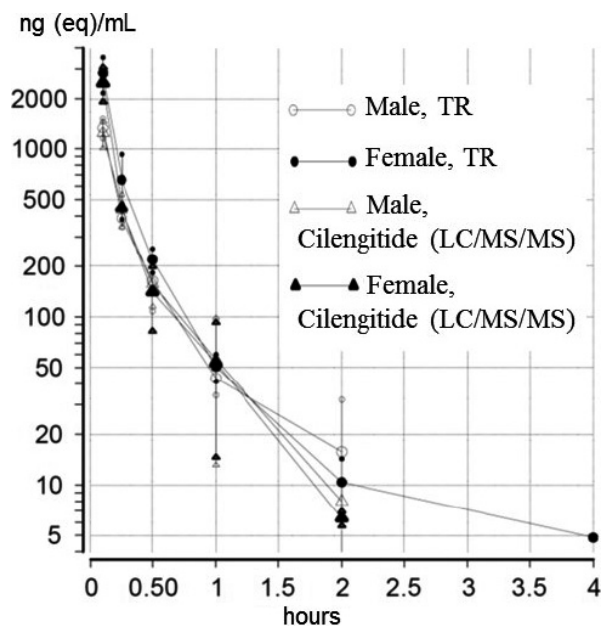


**Figure 2.** Mean ( $\pm$  CV%) plasma concentrations of total radioactivity (TR) and cilengitide after single i.v. administration of [ $^{14}$ C]-cilengitide (2.5 mg/kg) to male and female mice ( $n = 3$ /time-point).

tions then declined rapidly in a similar manner to those observed for radioactivity to 439 and 448 ng/mL (m/f) after 0.25 h, then to 8 and 6.3 ng/mL after 2 h (Fig. 2). The plasma  $t_{1/2}$  was short in both sexes (0.32 and 0.30 h). Clearance of cilengitide was high in male and female mice (5.68 and 3.20 L/h/kg) representing nominally 105% and 60% of hepatic blood flow (hbf), respectively, and indicating significant contribution of hepatic clearance to the total clearance of the drug in mouse. The apparent  $V_{d_{ss}}$  in both sexes was small (1.6 and 0.56 L/kg). As observed with plasma radioactivity, the  $AUC_{0-\infty}$  value for parent drug in females was approximately twice that of males (781 vs. 440 ng/mL/h). The values in males and females accounted for approximately 86% and 94% of the corresponding AUC values observed for plasma radioactivity, which is pretty consistent with limited metabolism in the mouse and also considering precision and accuracy of bioanalytical methods applied.

### Distribution

Following i.v. administration, [ $^{14}$ C]-cilengitide related radioactivity was rapidly distributed into mouse tissues within 0.1 h, as determined by tissue excision. Concentrations of radioactivity in plasma from the tissue distribution decreased rapidly from 2360 ng eq./mL (females) and 1970 ng eq./mL (males) at 0.1 h postdose to 4.2 and 5.1 ng eq./mL after 8 h of dosing. Concentrations and profiles of plasma radioactivity were similar to those

observed in the mouse PK study detailed above. Peak concentration in erythrocytes decreased from 195 and 132 ng eq/g in males and females to less than the limit of quantification at 8 h, indicating low uptake of radioactivity into the cellular compartment of whole blood.

The highest concentrations of radioactivity in male and female animals distributed into the liver (mean; 25450 ng eq/g), kidneys (8950 ng eq/g), skin (1693 ng eq/g), and muscles (413 ng eq/g), and represented 54.4, 4.7, 6.6, and 14.9% of the radioactive dose, respectively (total = 81%). In males and females, mean concentrations at 0.1 h after dosing in the adrenals, heart, and brain were 765, 627, and 272 ng eq/g, respectively, and by 8 h were low or nondetectable. At this time, levels in the ovaries and uterus (1324 ng eq/g) were about 2 times higher compared to testes (including epididymides and glandular vesicularis: 563 and 617 ng eq/g), but up to 3.5 times lower than those in plasma, indicating limited distribution into these tissues. After 8 h, concentrations in these organs were about 6–14 times higher and after 24 h about two times higher (testes, gl. vesicularis) than those observed in plasma. Levels in ovaries and uterus were nondetectable. At 24 h postdose, radioactivity decreased to very low, if at all detectable levels, with small amounts only found in testes, kidney, livers, lung, heart, and blood. At this time, only 0.8 and 0.4% of the dose was found in the carcasses of males and females.

These observations were confirmed in a study investigating the distribution properties of [ $^{14}$ C]-cilengitide in pigmented mice in order to support a [ $^{14}$ C]-mass balance study in human. Total radioactivity was mainly found in the excretory organs such as liver, gall bladder, GI tract, kidney, and urinary bladder. No prolonged binding of radioactivity to pigmented areas such as the eyes or the skin was detected, indicating that no relevant melanin binding occurred.

As observed in the quantitative tissue distribution study, the organs of excretion (liver, kidneys, and intestine) contained the highest concentrations of radioactivity at 0.1 h postdose (Fig. 3), as determined by whole-body autoradiography. Radioactivity was very rapidly cleared within 1 h of dosing, with levels of radioactivity only visible in the kidneys and intestine (Fig. 4), and after 8 h only in the large intestine, which is consistent with the very short elimination half-life observed for radioactivity and parent compound in mouse plasma.

### Metabolism

The major component circulating in mouse plasma was unchanged drug, which accounted for >85% of the sample radioactivity in both sexes (Fig. 5). A number of minor radioactive components were observed only in the

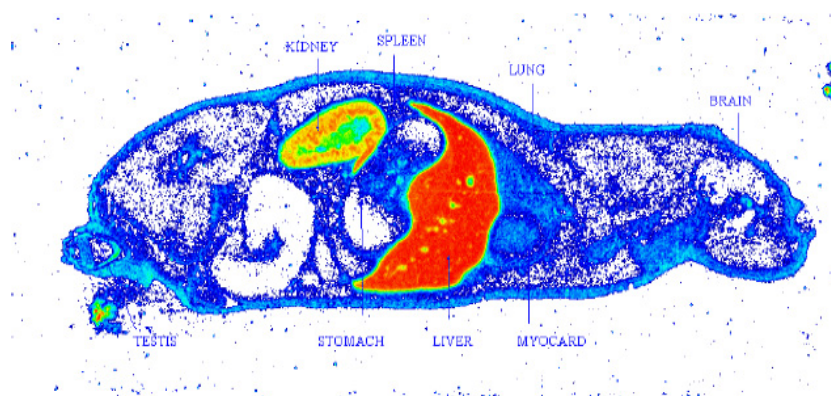


**Figure 3.** Distribution of radioactivity in the male mouse (NMRI) at 0.1 h after i.v. administration of [ $^{14}\text{C}$ ]-cilengitide. *blue*, low concentrations; *red*, high concentrations of radioactivity.

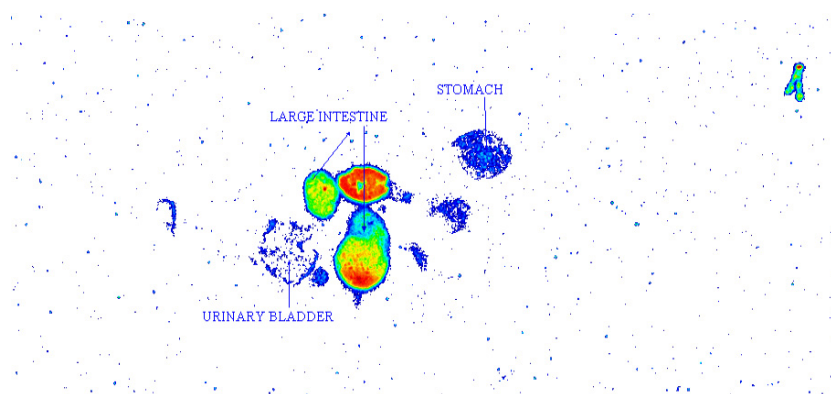


**Figure 4.** Distribution of radioactivity in the male mouse (NMRI) at 8 h after i.v. administration of [ $^{14}\text{C}$ ]-cilengitide. *blue*, low concentrations; *red*, high concentrations of radioactivity.

0.25 h samples, which could not be identified structurally. The amount of radioactivity remaining in the protein precipitate after plasma extraction varied between 6 and 12%. In male and female animals, 7.5 and 31% of the radioactive dose was recovered in urine within 24 h of dosing, with unchanged drug accounting for approximately 87–90% of the sample radioactivity (7 and 28% dose). No other radioactive components were detected (Fig. 6). More than 79% of the sample radioactivity in feces of both sexes was extractable, the remainder being recovered in the residues. In both sexes, unchanged drug represented more than 87% of the extractable radioactivity, equivalent to 87.2 and 66.2% of the administered dose in males and females (Fig. 7). No other radioactive components were detected.

### Excretion

Most of the radioactive dose (i.v.) in males and females was excreted in the feces (85.0 and 64.5%) within 24 h of dosing, presumably via biliary secretion (Table 3). Urine

accounted for a further 7.5 and 31.0% in males and females. Only 0.2% of the administered dose remained in the carcasses at the end of the 120-h study period, which is consistent with rapid elimination of the drug and its metabolites from the mouse.

## Monkey

### Pharmacokinetics

Mean concentrations of plasma radioactivity (8500 and 4230 ng eq/mL) in *Cynomolgus* monkey ( $n = 3$ ) declined rapidly between 0.1 and 0.5 h after i.v. dose administration (about 50%) and by 8 h represented only 0.6% of peak values (47.6 ng eq./mL; Fig. 8). The plasma radioactivity half-life ( $t_{1/2}$ ) was 1.2 h, although a further phase showing slower elimination was observed in one animal ( $t_{1/2}$ : 14.5 h). Mean concentrations of parent drug also decreased rapidly (by 48%) from 7020 to 3400 ng/mL between 0.1 and 0.5 h of dosing and to 24.6 ng/mL after 8 h (0.4% peak; Fig. 8). The apparent plasma elimination

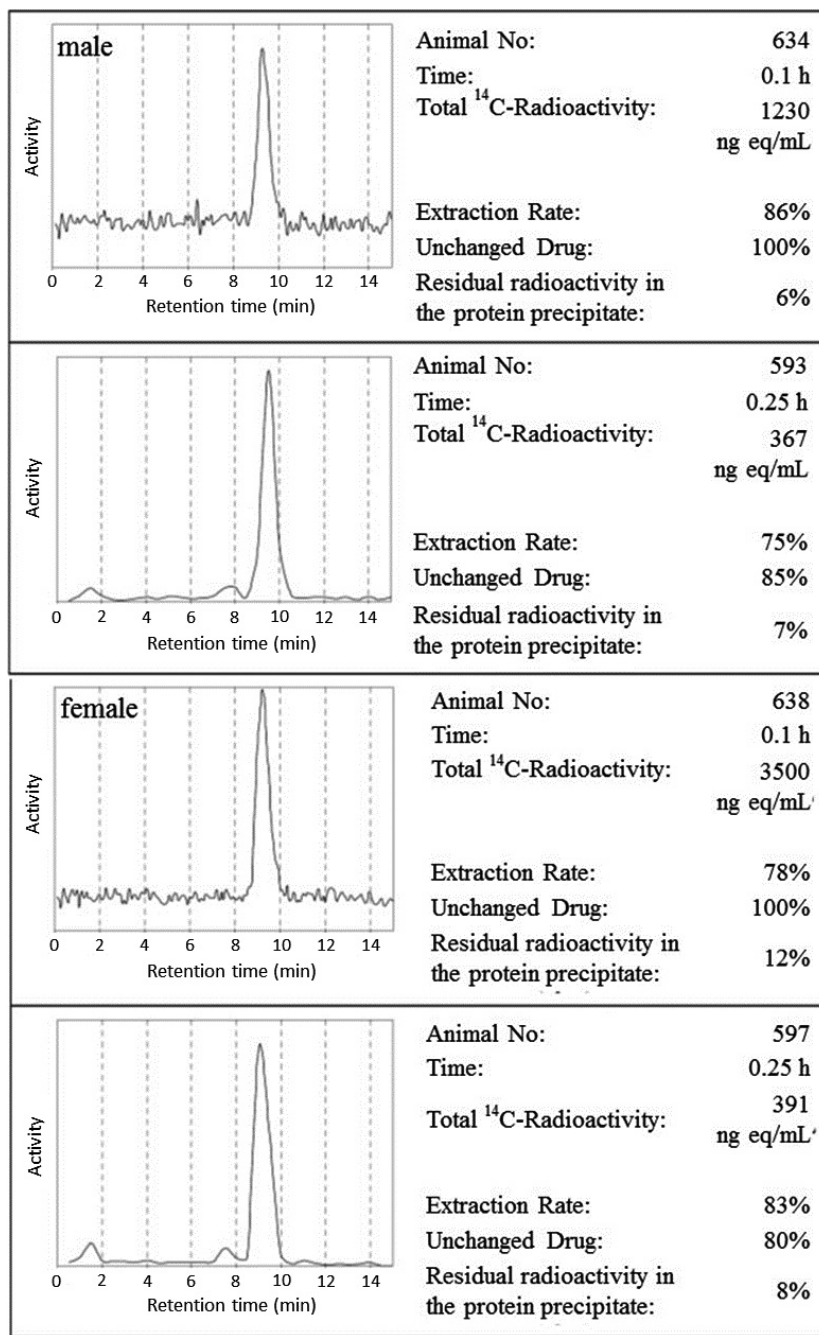


**Figure 5.** Radio- high-performance liquid chromatography (HPLC) profiles of plasma after i.v. administration of [<sup>14</sup>C]-cilengitide (2.5 mg/kg) to male and female mice (*N* = 1/gender/time-point).

for cilengitide (1.1 h) was similar to that observed for radioactivity and indicates that metabolites are not rate limiting in the elimination of the drug. The mean AUC<sub>0-∞</sub> value for cilengitide represented 69% of the corresponding AUC value observed for plasma radioactivity (6460 vs. 9390 (ng/mL) × h). In contrast to the mouse, mean clearance in monkey was low (0.32 L/h/kg),

representing only 12% of hbf. The apparent Vd<sub>ss</sub> as seen in mouse was low (0.35 L/kg).

### Metabolism

Following HPLC analysis of monkey plasma (0.1, 0.5, 1, 2, and 4 h), unchanged drug represented the entire

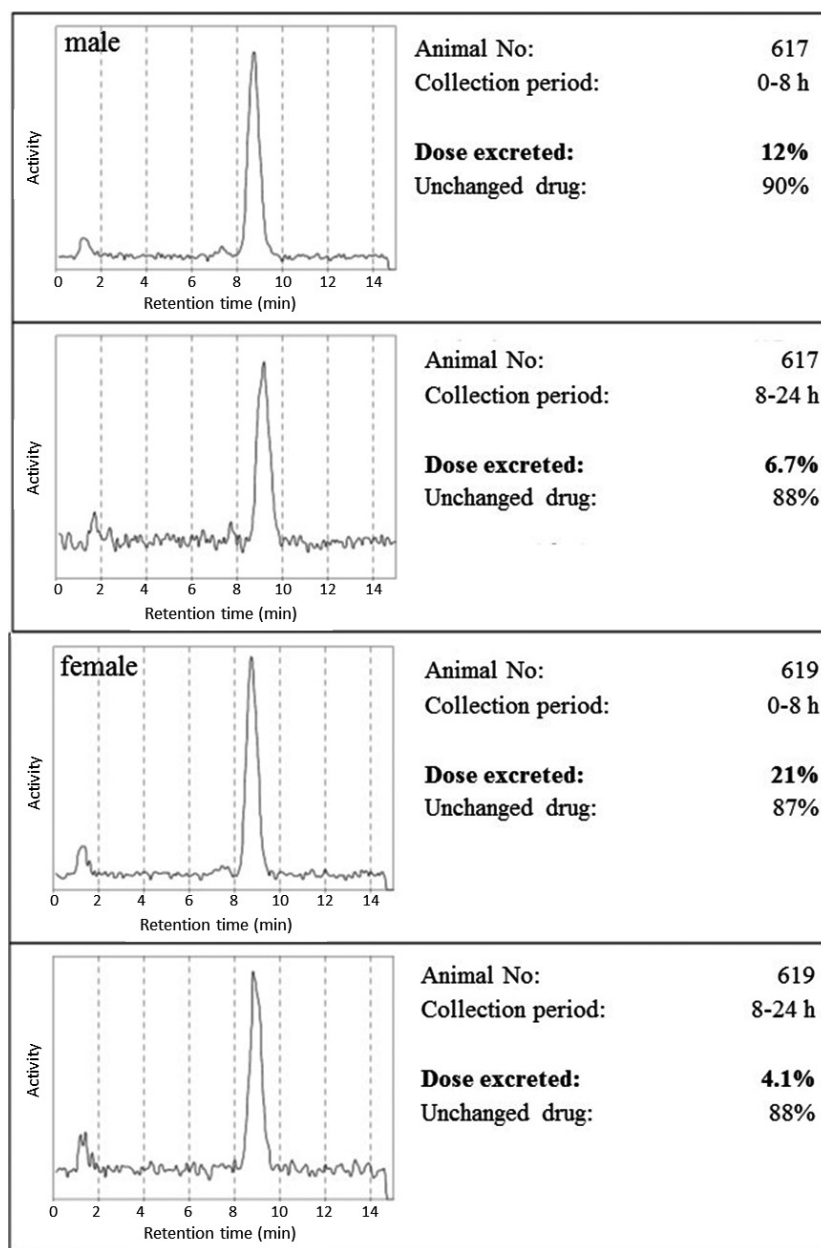


**Figure 6.** Radio- high-performance liquid chromatography (HPLC) profiles of urine after i.v. administration of [ $^{14}\text{C}$ ]-cilengitide (2.5 mg/kg) to male and female mice ( $N = 1/\text{gender}$ ).

extractable radioactivity (~100%; Fig. 9). The amount of radioactivity remaining in the precipitate after extraction varied between 7.4 and 28.6%. These samples were not profiled by radio-HPLC for metabolites.

Unchanged drug accounted for more than 90% of the sample radioactivity in urine, accounting for about 50% of the administered i.v. dose. No metabolites of [ $^{14}\text{C}$ ]-cilengitide were evident in urine (Fig. 10). Approximately 37% of the radioactive dose was excreted via the feces. However, only about 20% of the fecal

sample radioactivity was extractable, the remainder being recovered as [ $^{14}\text{C}$ ]- $\text{CO}_2$  after combustion of the non-soluble constituents. The HPLC pattern of the fecal extracts showed a relatively high portion of metabolites with large interindividual differences (Fig. 10). This pattern was not observed in either the urine or the plasma profiles. The significance of this observation is not known at present, but these metabolites may be products of biotransformations caused by the microflora in the monkey intestine.

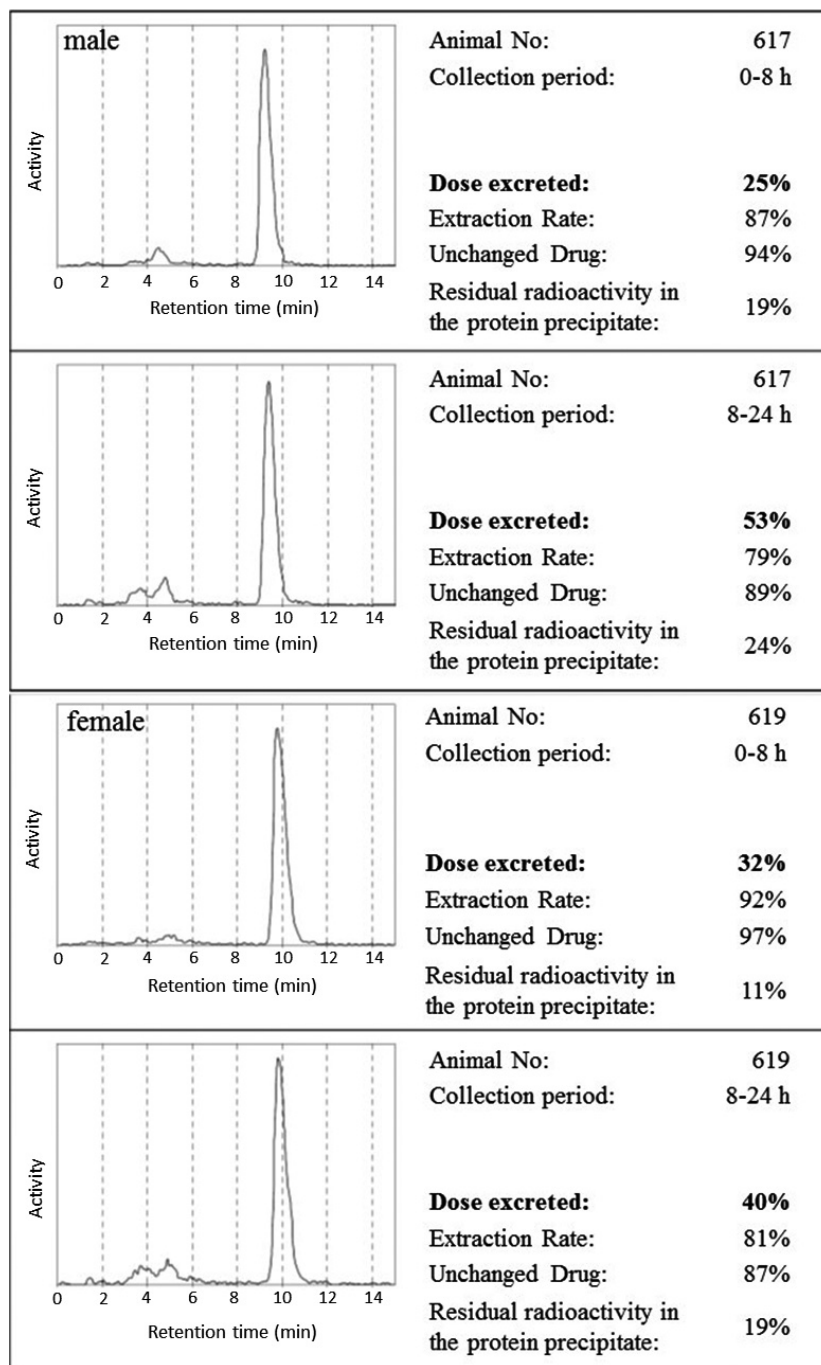


**Figure 7.** Radio- high-performance liquid chromatography (HPLC) profiles of feces after i.v. administration of [<sup>14</sup>C]-cilengitide (2.5 mg/kg) to male and female mice (*N* = 1/gender).

**Excretion**

Means of 56.0 and 17.9% of the radioactive dose was recovered in urine and feces after 24 h of dosing (Table 3). At the end of 120-h study period, the corresponding values were 58.1 and 36.5% dose, respectively (total dose: 94.7%).

**Rat**

**Pharmacokinetics**

Following intravenous bolus injection of 2.5 mg/kg cilengitide to rats, plasma levels at the initial sampling time

**Table 3.** Excretion of radioactivity in urine and feces following i.v. administration of [<sup>14</sup>C]-cilengitide to mouse, monkey, and human.

Species	Excreta	0–24 h(% dose)		0–120 h (% dose)	
		Male	Female	Male	Female
Mouse <sup>1</sup>	Urine	7.5	31.0	8.2	31.7
	Feces	85.0	64.5	87.2	66.2
	Total	92.5	95.5	95.4	97.9
Monkey <sup>2</sup>	Urine	ND	56.0	ND	58.1
	Feces	ND	17.9	ND	36.5
	Total	ND	73.9	ND	94.7
Human <sup>3</sup>	Urine	~78	ND	79.0 <sup>4</sup>	ND
	Feces	~9.0	ND	15.5 <sup>4</sup>	ND
	Total	~87	ND	94.5 <sup>4</sup>	ND

Human data is referred to Becker et al. 2015.

ND, not determined.

<sup>1</sup>*n* = 3.

<sup>2</sup>*n* = 2.

<sup>3</sup>*n* = 5.

<sup>4</sup>0–144 h.

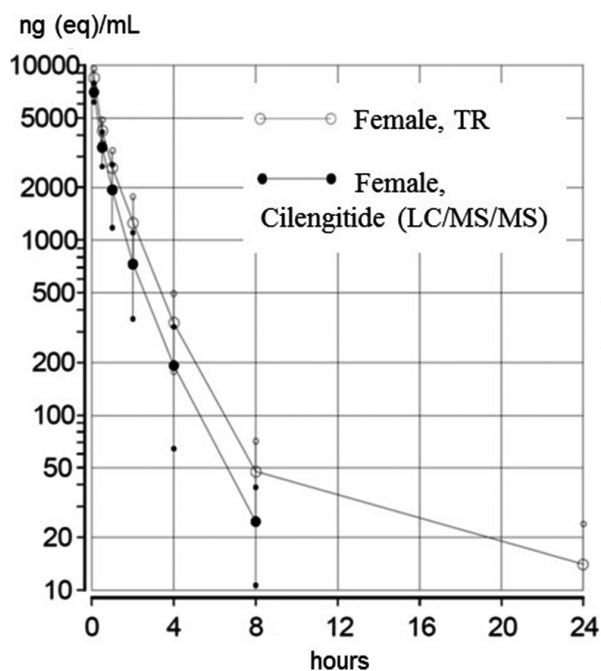


**Figure 8.** Mean (+ CV%) plasma concentrations of total radioactivity (TR) and cilengitide after single i.v. administration of [<sup>14</sup>C]-cilengitide (2.0 mg/kg) to female cynomolgus monkey (*n* = 3).

(0.1 h) were high (5360–5870 ng/mL). Plasma concentrations of unchanged drug then declined rapidly resulting in a short half-life ( $t_{1/2}$ : 0.24–0.50 h) similar to that of the mouse. In consequence, clearance of cilengitide was about 0.98 L/h/kg, equivalent to approximately 20% of hepatic blood flow (hbf) in this species. The apparent

volume of distribution at steady state ( $V_{d,ss}$ ) was limited (0.34 L/kg), virtually representing the vascular space.

## Rabbit

### Pharmacokinetics

Plasma concentrations of parent drug were quantified before, during and after intravenous infusion. At the end of infusion, mean plasma concentrations were 34,200–38,500 ng/mL at the low dose level (50 mg/kg). The apparent half-life after the end of infusion of approximately 0.6 h was short in comparison to the daily administration interval. In the 450 mg/kg dose group, the apparent half-life was somewhat longer (ca ~ 1 h) when compared to the low and the intermediate dose levels. This observation could suggest that elimination processes are at or close to the saturation level at high doses and associated plasma concentrations.

Thus, plasma clearance of cilengitide was low in female rabbits (0.36 L/h/kg) in comparison to hbf (ca 15%), which is more similar to monkey than mouse. As observed in the mouse and monkey, the apparent  $V_{d,ss}$  was also low in the rabbit (0.40 L/kg).

### Allometric scaling

Simple allometric scaling based on four species was used to predict the clearance and volume of distribution (at steady state) in humans (Table 4). The predicted PK parameters were  $CL = 0.087$  L/h/kg,  $V_{d,ss} = 0.238$  L/kg leading to a half-life ( $t_{1/2}$ ) of approximately 2 h (Tables 5 and 6), which were remarkably similar to those observed in a human volunteer study ( $CL = 0.09 \pm 0.02$  L/h/kg,  $V_z = 0.31 \pm 0.04$  L/kg and  $t_{1/2} = 2.5 \pm 0.44$  h). Predicted human ranges of approximately twofold are presented in Table 6.

## In vitro incubations with cilengitide

### Evaluation of hepatobiliary disposition

The use of the B-CLEAR<sup>®</sup> culture system in this study was considered an appropriate in vitro model to investigate the hepatic metabolism of a very low permeable drug such as cilengitide due to the maintained expression of uptake and efflux transporters together with the hepatic drug metabolic enzymes. Hepatobiliary disposition of the positive control taurocholate confirmed the transporter functionality of the hepatocytes from both species (Tables 7 and 8).

In mouse hepatocytes, uptake of cilengitide was fairly robust and biliary efflux was modest with a BEI of about

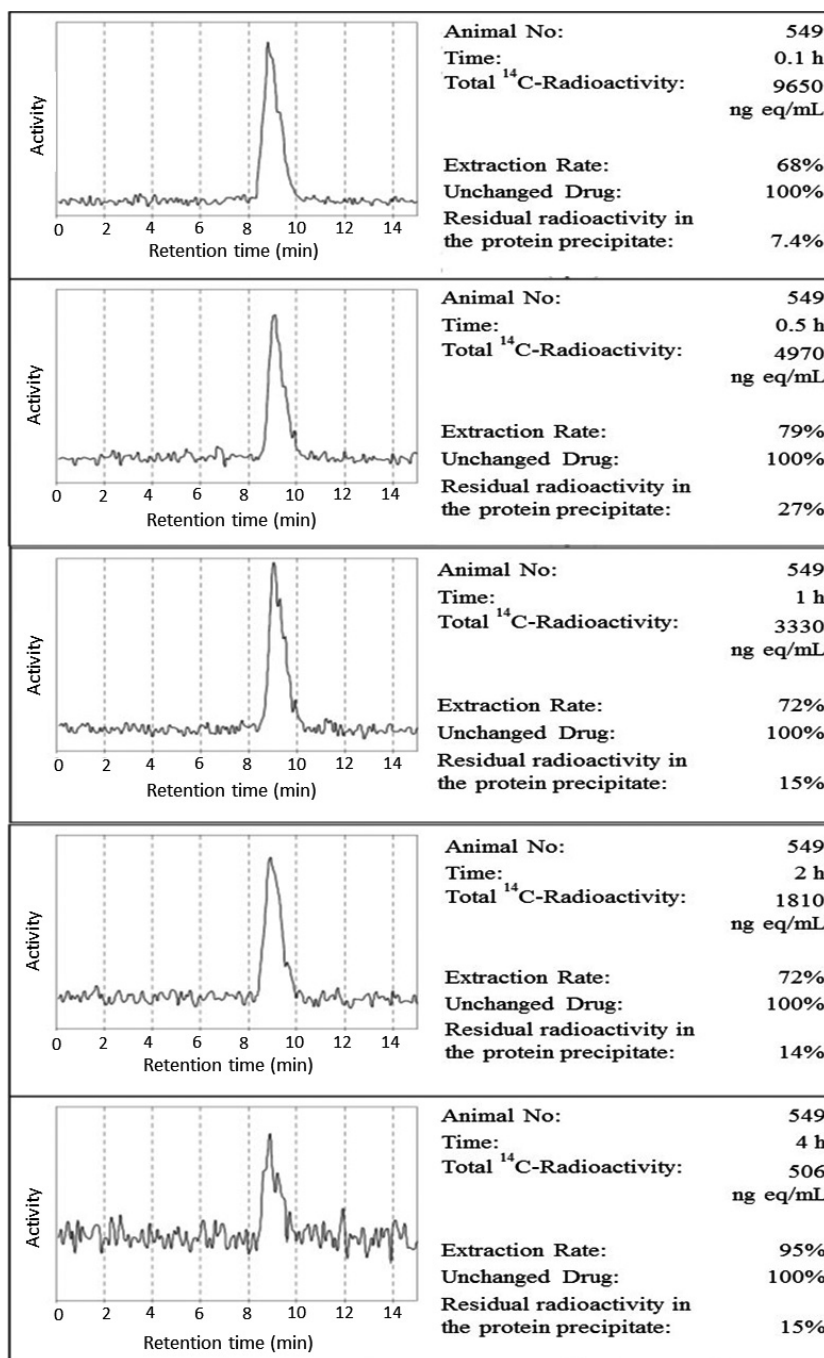


**Figure 9.** Radio- high-performance liquid chromatography(HPLC) profiles of plasma after i.v. administration of [<sup>14</sup>C]-cilengitide (2.0 mg/kg) to female cynomolgus monkey (N = 1).

30–40% (Table 9). The intracellular concentrations ( $C_{ic}$ ) were determined to be 4.13 and 219  $\mu\text{mol/L}$  after exposure towards 10 and 250  $\mu\text{mol/L}$  cilengitide, respectively. In human hepatocytes, the total and cellular accumulation of cilengitide was much lower compared to mouse hepatocytes (Table 10). The intracellular concentration of cilengitide in human hepatocytes was

0.926  $\pm$  0.386  $\mu\text{mol/L}$  and 16.1  $\pm$  3.6  $\mu\text{mol/L}$  after exposure at 10 and 250  $\mu\text{mol/L}$ , respectively, with  $C_{ic}/C_{ec}$  (extracellular concentration) ratios in the range of 0.09–0.06. The biliary efflux (as determined by BEI and  $CL_{bil}$ ) was negligible. These data indicate a clear species difference in the hepatobiliary disposition of cilengitide between mouse and human hepatocytes.

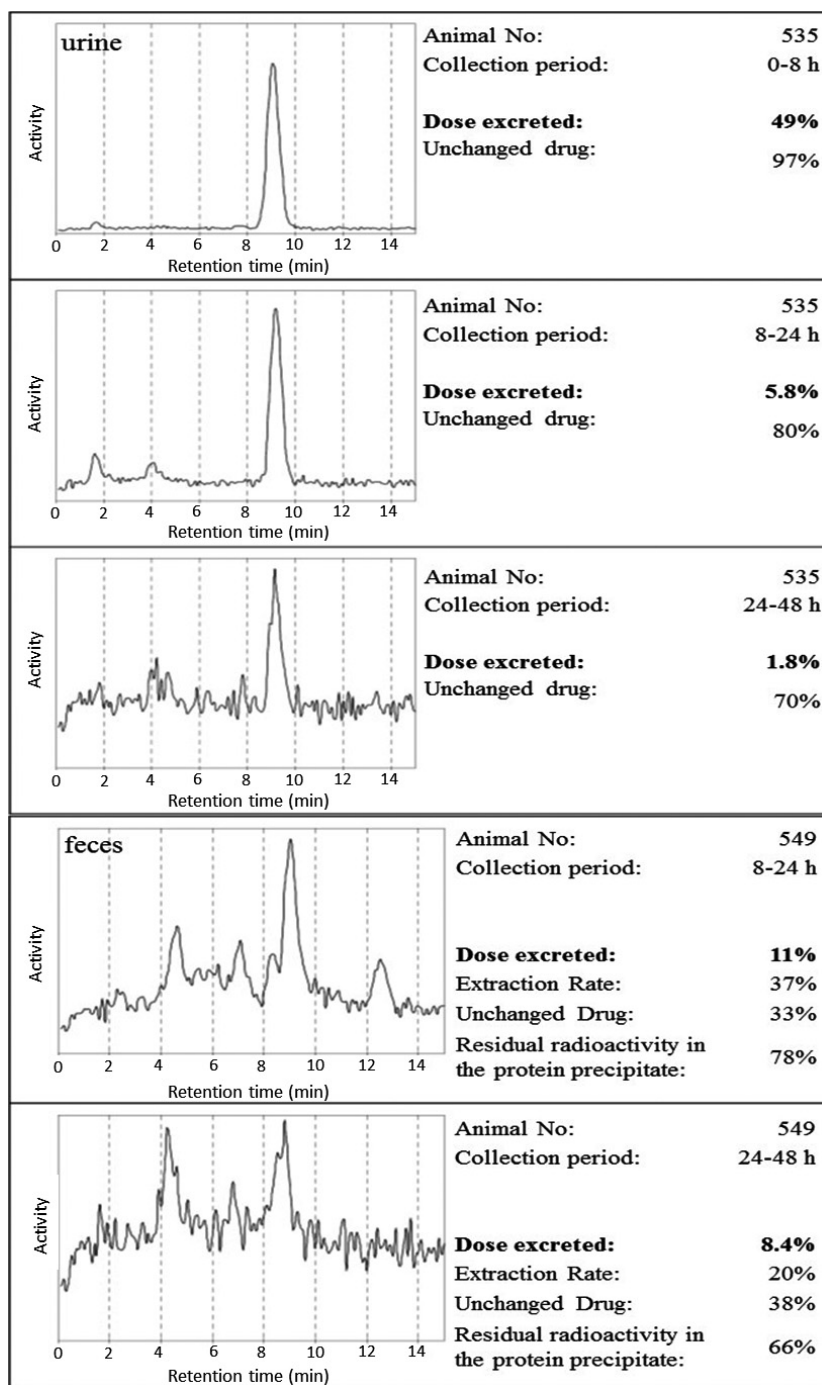


**Figure 10.** Radio- high-performance liquid chromatography (HPLC) profiles of urine and feces after i.v. administration of [ $^{14}\text{C}$ ]-cilengitide (2.0 mg/kg) to female cynomolgus monkey ( $N = 1$ ).

### Uptake into hepatocytes

The results from the sandwich-cultured hepatocytes model suggested that the intracellular accumulation of cilengitide was limited in human hepatocytes. To confirm

this observation, uptake of cilengitide (10  $\mu\text{mol/L}$ , 250  $\mu\text{mol/L}$ , and 10  $\text{mmol/L}$ ) into human hepatocytes was measured in suspension (Fig. 11). To investigate a potential of saturation of active transport, it was also examined at 10  $\text{mmol/L}$ , an excess concentration.

**Table 4.** Predicted plasma clearance in human using simple allometry

Clearance	Log(BW)	Log(CL)
Mouse	-1.699	-1.12
Rat	-0.658	-0.668
Monkey	0.491	-0.048
Rabbit	0.633	0.195
Human	1.78	0.713
intercept		-0.244
slope		0.540
R <sup>2</sup>		0.981
Predicted Human CL (L/h)		5.20
Observed Human CL (L/h)		5.32

Human data is referred to Becker *et al.* 2015.

**Table 5.** Vss estimations in human for cilengitide.

Volume	Log(BW)	Log(Vss)
Mouse	-1.699	-1.82
Rat	-0.658	-1.13
Monkey	0.491	0.00
Rabbit	0.633	0.236
Human	1.78	1.155
intercept		-0.408
slope		0.879
R <sup>2</sup>		0.988
Predicted Human Vss (L)		14.3
Observed Human Vss (L)		19.4

Human data is referred to Becker *et al.* 2015.

**Table 6.** Range of predicted PK parameters in human based on simple allometry.

	Vss, predicted (L/kg)			
	-2 fold	Vss	+2 fold	
Predicted t <sub>1/2</sub> (h)	0.12	0.24	0.48	
CL, predicted (L/h/kg)	-2 fold	0.043	1.9	3.9
	CL	0.096	1.0	2.1
	+2 fold	0.172	0.5	1.0

**Table 7.** Positive control for transporter function in sandwich cultured hepatocytes (mouse).

	Total accumulation (pmol/mg)	Cellular accumulation (pmol/mg)	BEI (%)	CL <sub>biliary</sub> (mL/min/kg)
Control Probe				
TCA	215 ± 23	150 ± 28	30.5	66.8

Accumulation data are presented as mean ± SD of triplicate wells; BEI and CL<sub>biliary</sub> are derived values. Experiment performed using a single NMRI mouse liver.

TCA: taurocholate.BEI, biliary excretion index.

Distribution of cilengitide into human hepatocytes was almost complete after 1–4 min. Only low quantities of cilengitide were found in the hepatocyte fraction after the respective incubation times (1–30 or 90 min.). These results indicate that the uptake of cilengitide into human hepatocyte was minor and showed no clear dependency on drug concentration. A dependency would have been expected in the case of an active uptake substrate involving saturation of active uptake at high concentrations. The presence of the inhibitor cocktail showed no relevant inhibition on the distribution of cilengitide into hepatocytes substantiating the findings above.

## Discussion

Cilengitide belongs to a new class of investigational targeted anticancer therapies which was under clinical development (Phase III) by Merck as a potential novel *i.v.* agent for anticancer therapies. It has now been withdrawn from the treatment of cancer patients diagnosed with glioblastoma due to a lack of efficacy (Soffietti *et al.* 2014). Cilengitide exhibits low passive permeability in the Caco-2 model (see Supporting Information), which is consistent with its physicochemical properties (MW: 588.67 g/mol; log Po/w = -2.0; high solubility). According to the BDDCS classification of Wu and Benet (2005), cilengitide is considered a class III molecule and therefore is expected to have low metabolism with high unchanged drug renal/biliary secretion.

In fact, *in vitro* metabolism studies showed that cilengitide is poorly metabolized by liver microsomes of mice, monkeys, and humans (see Supporting Information), as well as by cultured hepatocytes from rat and human. Current *in vivo i.v.* studies showed that the major component circulating in mouse and monkey plasma was unchanged cilengitide, accounting for >85% of total drug-related material (Figs. 7, 10). A number of minor radioactive metabolites were observed only in mouse plasma, but could not be structurally identified.

Noticeably, the disposition pattern of cilengitide showed a profound species difference with high renal excretion of the parent drug in female Cynomolgus monkey (~50% dose), but not in male and female mice (7 and 28% dose; Figs. 8, 9, 12 and 11). Following *i.v.* administration in mice, a very high uptake and biliary secretion of cilengitide was observed (87 and 66% dose), which is supported by tissue distribution and metabolism studies with [<sup>14</sup>C]-cilengitide in that species. In contrast in monkey, biliary secretion of cilengitide was lower (36.5% dose). The metabolite pattern of feces extracts showed a relatively high portion of metabolites and large interindividual differences (Fig. 10), however, only 20% of the sample radioactivity could be extracted from the

**Table 8.** Positive control for transporter function in sandwich cultured hepatocytes (Human).

Control probe	<i>n</i>	Total accumulation (pmol/mg)	Cellular accumulation (pmol/mg)	BEI (%)	CL <sub>biliary</sub> (mL/min/kg)
TCA	1	55.3 ± 5.7	30.7 ± 2.8	44.6	7.16
	2	89.7 ± 3.6	23.2 ± 1.9	74.2	19.3
	3	161 ± 12	53.9 ± 2.0	66.5	31.0
Mean ± standard error		102 ± 31	35.9 ± 9.2	61.7 ± 8.9	19.2 ± 6.9

Accumulation data are presented as mean ± SD of triplicate wells; BEI and CL<sub>biliary</sub> are derived values. Experiment performed using three separate human liver preparations.

TCA: taurocholate, BEI, biliary excretion index.

*n*: donor number.

**Table 9.** Hepatobiliary disposition of cilengitide in sandwich cultured hepatocytes (Mouse).

Cilengitide concentration (μmol/L)	Total accumulation Avg. (pmol/mg)	Cellular accumulation Avg. (pmol/mg)	Intracellular concentration (μM)	BEI (%)	CL <sub>biliary</sub> (mL/min/kg)
10	47.1 ± 1.7	33.3 ± 1.4	4.13	29.3	0.701
250	3115 ± 32	1768 ± 14	219	43.3	2.74

Incubation time: 20 min.

Accumulation data are presented as mean ± standard deviation of triplicate wells; Intracellular Concentration, BEI and CL<sub>biliary</sub> are derived values. Experiment performed using a single NMRI mouse liver.

**Table 10.** Hepatobiliary disposition of cilengitide in sandwich cultured hepatocytes (Human).

Cilengitide concentration (μM)	<i>n</i>	Total accumulation Avg. (pmol/mg)	Cellular accumulation Avg. (pmol/mg)	Intracellular concentration (μM)	BEI (%)	CL <sub>biliary</sub> (mL/min/kg)
10	1	14.0 ± 1.5	13.7 ± 1.8	1.70	2.42	0.005
10	2	4.27 ± 0.46	4.17 ± 0.33	0.52	2.30	0.004
10	3	5.44 ± 3.31	4.53 ± 0.38	0.56	16.6	0.013
Mean±Standard Error		7.90 ± 3.07	7.47 ± 3.12	0.926 ± 0.386	7.12 ± 4.76	0.007 ± 0.003
250	1	230 ± 28	183 ± 27	22.7	20.4	0.028
250	2	92.1 ± 5.7	84.0 ± 12.1	10.4	8.75	0.005
250	3	145 ± 5.9	122 ± 14	15.2	15.6	0.013
Mean±Standard Error		156 ± 3	130 ± 29	16.1 ± 3.6	14.9 ± 3.4	0.015 ± 0.007

Incubation time: 20 min.

Accumulation data are presented as mean ± standard deviation of triplicate wells; Intracellular Concentration, BEI and CL<sub>biliary</sub> are derived values. Experiment performed using three separate human liver preparations.

*n*: donor number; BEI, biliary excretion index.

feces. These degradation products may be the result of biotransformation by the intestinal microflora or enzymes present in the intestinal wall. In *Cynomolgus* monkey, about 74% of the i.v. dose was recovered in the excreta within 24 h (95% after 120 h), which was lower than observed in mouse, presumably reflecting the lower CL (Table 11). This is in accordance with the metabolite pattern in urine and plasma, indicating that cilengitide was mainly eliminated as unchanged drug.

Plasma clearance of cilengitide in male and female mice was high (5.68 and 3.20 L/h/kg), representing 105% and 60% of hbf, respectively. In contrast, CL in

monkey was low (0.3 L/h/kg), representing only 12% of hbf. The PK of total radioactivity in mouse and monkey plasma was similar to those observed for parent drug, confirming little or no metabolism in either species. This indicates efficient clearance by nonmetabolic routes, which are fast in mice and slower in monkey. The V<sub>d,ss</sub> was low in both species (0.32–1.6 L/h/kg) indicating limited distribution of the drug (and metabolites) from the central compartment into the tissues. Plasma pharmacokinetics observed in rats and rabbits appeared to be consistent with the other primary preclinical species.

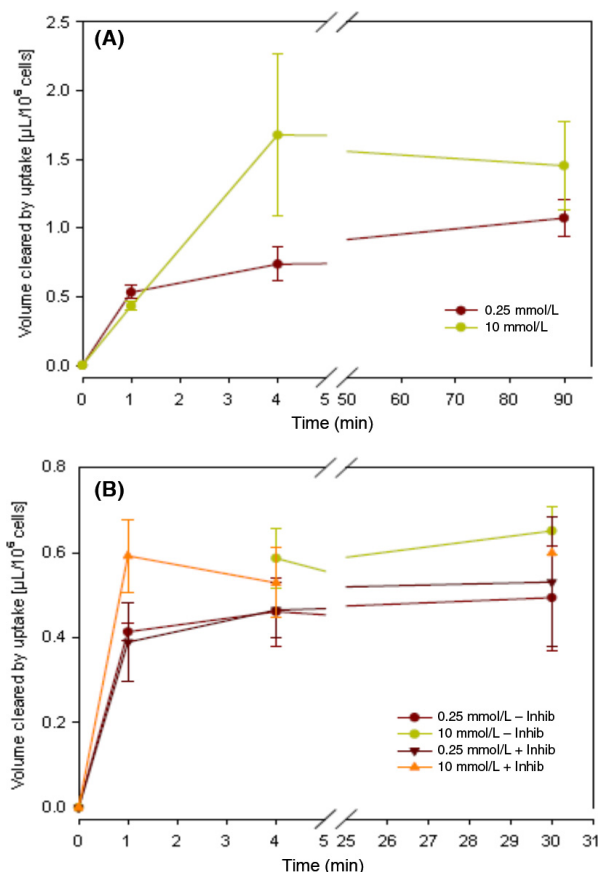


**Figure 11.** Uptake of cilengitide into human suspension hepatocytes. (A). at 250  $\mu\text{mol/L}$  and 10 mmol/L ( $n = 2-3$ ), b) at 10  $\mu\text{mol/L}$  and 250  $\mu\text{mol/L}$  in presence or absence of inhibitor cocktail ( $n = 2-3$ ), except for the data point at 30 min incubation of 10  $\mu\text{mol/L}$  cilengitide with inhibitor cocktail, which was  $n = 1$ .

A recent ADME study in human volunteers (Becker et al. 2015) with [ $^{14}\text{C}$ ]-cilengitide (i.v. 2000 mg; 3397  $\mu\text{mol}$ ) showed that the PK and plasma profiles for radioactivity and unchanged drug were almost superimposable (Fig. 12), as was the case with animals, suggesting that little or no formation- or elimination-rate limiting metabolites were generated. Plasma radioactivity and cilengitide concentrations decreased rapidly with a mean  $t_{1/2}$  of approximately 2.2–2.5 h resulting from the low clearance and the low volume of distribution of cilengitide in human (0.09 L/h/kg and 0.31 L/kg). PK of cilengitide, including renal clearance of the drug, was in agreement with other studies in healthy volunteers and cancer patients (Eskens et al., 2003 and O'Donnell et al. 2010).

Contrary to the mouse, most of the radioactive dose in human was renally cleared as unchanged drug (77.5%). Renal clearance of cilengitide was below the creatinine clearance determined in each subject, suggesting passive

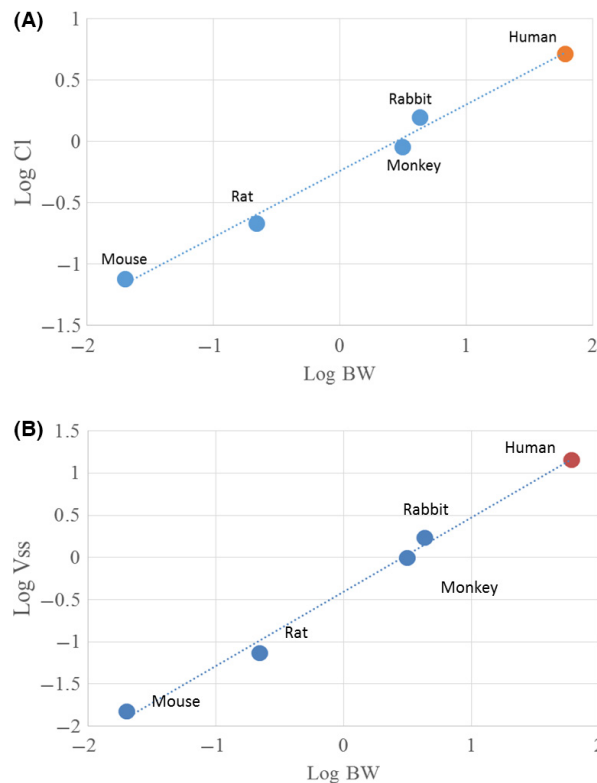


**Figure 12.** 4-species allometric scaling of cilengitide on CL (A) and V<sub>ss</sub> (B). Human data is referred to Becker et al. 2015.

**Table 11.** Physiological parameters and clearance data used for allometry studies with cilengitide.

Species	V <sub>ss</sub> (L/kg)	Plasma CL (L/h/kg)	t <sub>1/2</sub> (h)	BW (kg)
Mouse	0.76	3.81	0.34	0.02
Rat	0.34	0.98	0.50	0.22
Monkey	0.32	0.29	1.25	3.1
Rabbit	0.40	0.36	0.61	4.3
Human				60

glomerular filtration in the kidney without active secretion into urine. Elimination into bile and/or the intestine constitutes a minor elimination route of cilengitide in humans, as 15.5% and 79% of radioactive dose were found in feces and urine, respectively (Table 3). In agreement with animal results, parent compound was the only component found in human plasma (Fig. 13) and urine. In feces, two minor metabolites, M606-1 and M606-2 were identified: M606-1 was characterized as the linear pentapeptide D-Phe-N-MeVal-Arg-Gly-Asp and M606-2 as Asp-D-Phe-N-MeVal-Arg-Gly. Generation requires cleavage of the parent cyclic peptide on either side of the Asp moiety. Such catalytic activity is known to reside in intestinal peptidases or in peptidases from fecal bacteria,

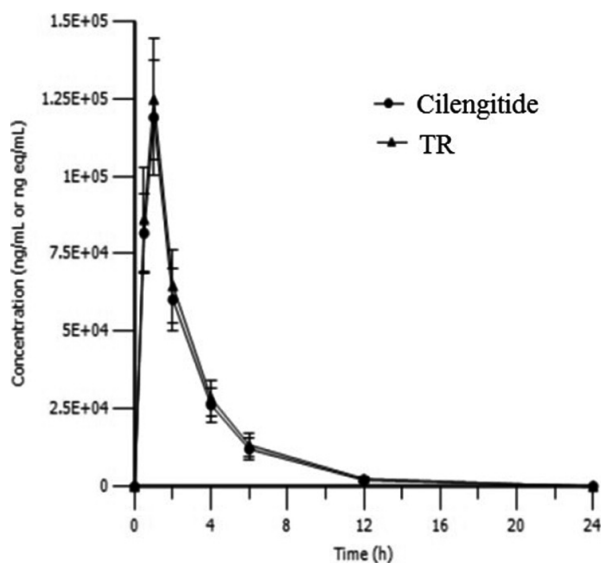


**Figure 13.** Mean plasma concentration–time profiles of cilengitide and total radioactivity (TR) after single i.v. infusion to healthy volunteers. Subjects received a single dose of 2.1 MBq of [ $^{14}\text{C}$ ]-cilengitide spiked into 250 mL of 2000 mg of unlabeled cilengitide solution as an intravenous infusion over 1 hour. This result is referred to Becker et al. 2015.

and thus indicates formation locally in enterocytes or in the intestinal lumen subsequent to excretion of unchanged cilengitide into feces (Wallace 1997).

Interestingly, the predicted PK values based on allometric scaling ( $CL = 0.087 \text{ L/h/kg}$ ,  $V_d = 1.155 \text{ L/kg}$ , and  $t = 1.90 \text{ h}$ ) were very similar to those obtained from clinical studies in healthy volunteers and cancer patients (Fig. 12). Hence, allometric scaling did well predict the human PK although the large interspecies difference in the drug disposition mechanisms was masked.

Additional in vitro experiments were undertaken to better understand the species differences in disposition mechanisms. To this end, hepatobiliary disposition of cilengitide was investigated using sandwich-cultured mouse and human hepatocytes systems (Ghibellini et al. 2004, 2006, 2007). In mouse hepatocytes, the observed modest biliary efflux ( $BEI = 30\text{--}40\%$ ;  $C_{ic}/C_{ec}$ : 0.6–0.9) indicated significant prior uptake into those cells (Table 9). In human hepatocytes, however, the total and cellular accumulation of cilengitide was much lower ( $C_{ic}/C_{ec}$ : 0.08) and biliary efflux negligible, indicating lack of active uptake into hepatocytes (Table 10). These results clearly demonstrate the usefulness of the sandwich-cultured hepatocytes model to interpret the species difference in in vivo biliary disposition.

Previous in vitro transporter studies have shown that other cyclopeptides (phalloidin and  $\alpha$ -amanitin) with similar physicochemical properties as cilengitide

demonstrated a clear hepatic uptake mediated by OATPs (Fehrenbach et al. 2003 and Letschert et al. 2006). However, no active uptake of cilengitide was indicated in human hepatocytes (Fig. 11). Due to its hydrophilic character ( $\text{Log } P_{o/w} = -2.0$ ), it can be assumed that passive diffusion into cells plays a negligible role for cilengitide which is in accordance with its very low in vitro permeability (approximately 1.0 nm/sec) observed in Caco-2 cells (see Supporting Information). This result is also in agreement with the observations in sandwich-cultured human hepatocytes.

In summary, cilengitide is a class III molecule according to the BDDCS classification with no or little metabolism expected. No metabolites were detected in the systemic circulation of preclinical species and human. Cilengitide was essentially secreted unchanged via the renal and biliary routes, and although fecal metabolites were observed in the monkey, these are hypothesized to be a result of microfloral metabolism. Surprisingly, the extent of the renal and biliary secretion is highly species dependent, which is masked by the relative well conserved clearance across the species. The extent of renal excretion of cilengitide appears to increase with species evolution, that is, lowest in mouse, then monkey and human (10 vs. 56 vs.  $\sim 80\%$ ). In contrast, biliary secretion was highest in mouse and lowest in human, which were qualitatively demonstrated well using sandwich cultures of mouse and human hepatocytes. In human, active and passive uptake into the hepatocyte appears not to play a significant role in the distribution of the drug. Due to the low biliary secretion in human of cilengitide in vitro, the efflux transporter(s) involved could not be identified.

## Acknowledgements

We acknowledge Qualyst Transporter Solutions, LLC, 2810 Meridian Parkway, Durham, NC 27713, USA who conducted in vitro studies on the hepatobiliary disposition and metabolism studies with [ $^{14}\text{C}$ ]-cilengitide and who provided incubation specimens to XenoTech, LLC 16825 Lenexa, KS 66219, USA for metabolic activity analysis. We also thank Mr Reinhard Kunert for his work on the protein binding. We thank Mr. Jack Allen for the editorial support. We thank INSERM U505, Paris, France for providing the Caco-2 TC7 cells.

## Author Contributions

Participated in research design: Dolgos, Freisleben, Scheible, Galleman, and Fluck. Conducted experiments: Galleman, Krätzer, Yamagata, and Fluck. Contributed new reagents or analytic tools: Not applicable. Performed data analysis: Dolgos, Freisleben, Scheible, Galleman,

Krätzer, and Fluck. Wrote or contributed to the writing of the manuscript: Dolgos, Freisleben, Scheible, Galle-mann, Wimmer, Yamagata, and Fluck.

## Disclosure

None declared.

## References

- Albert JM, Cao C, Geng L, Leavitt L, Hallahan DE, Lu B (2006). Integrin  $\alpha v \beta 3$  antagonist cilengitide enhances efficacy of radiotherapy in endothelial cell and nonsmall-cell lung cancer models. *Int J Radiat Oncol Biol Phys* 65: 1536–1543.
- Aoudjit F, Vuori K (2001). Integrin signaling inhibits paclitaxel-induced apoptosis in breast cancer cells. *Oncogene* 20: 4995–5004.
- Becker A, von Richter A, Kovar A, et al. (2015). Metabolism and disposition of the  $\alpha v$ -integrin  $\beta 3/\beta 5$  receptor antagonist cilengitide, a cyclic polypeptide, in humans. *J Clin Pharmacol* 55: 815–824.
- Bradley DA, Daignault S, Ryan CJ, et al. (2011). Cilengitide (EMD 121974, NSC 707544) in asymptomatic metastatic castration resistant prostate cancer patients: A randomized phase II trial by the prostate cancer clinical trials consortium. *Invest New Drugs* 29: 1432–1440.
- Courter DL, Lomas L, Scatena M, Giachelli Cecilia M (2005). Src kinase activity is required for integrin  $\alpha v \beta 3$ -mediated activation of nuclear factor- $\kappa B$  (2005). *B. J Biol Chem*. 280: 12145–12151.
- Dechantsreiter MA, Planker E, Mathä B, et al. (1999). N-Methylated cyclic RGD peptides as highly active and selective  $\alpha v \beta 3$  integrin antagonists. *J Med Chem* 42: 3033–3040.
- Dolfi F, Garcia-Guzman M, Ojaniemi M, Nakamura H, Matsuda M, Vuori K (1998). The adaptor protein Crk connects multiple cellular stimuli to the JNK signalling pathway. *Proc Natl Acad Sci USA* 95: 15394–15399.
- Eskens FALM, Dumez H, Hoekstra R, Perschl A, Brindley C, Böttcher S, et al. (2003). Phase I and pharmacokinetic study of continuous twice weekly intravenous administration of cilengitide (EMD 121974), a novel inhibitor of the integrins  $\alpha v \beta 3$  and  $\alpha v \beta 5$  in patients with advanced solid tumours. *Eur J Cancer* 39: 917–926.
- Fehrenbach T, Cui Y, Faulstich H, Keppler D (2003). Characterization of the transport of the bicyclic peptide phalloidin by human hepatic transport proteins. *Naunyn-Schmiedeberg's Arch Pharmacol* 368: 415–420.
- Friess H, Langrehr JM, Oettle H, Raedle J, Niedergethmann M, Ditttrich C, et al. (2006). A randomized multi-center phase II trial of the angiogenesis inhibitor cilengitide (EMD 121974) and gemcitabine compared with gemcitabine alone in advanced unresectable pancreatic cancer. *BMC Cancer* 6: 285.
- Ghibellini G, Johnson BM, Kowalsky RJ, Heizer WD, Brouwer KL (2004). A novel method for the determination of biliary clearance in humans (2004). *AAPS J* 6: e33.
- Ghibellini G, Leslie EM, Brouwer KL (2006). Methods to evaluate biliary excretion of drugs in humans: an updated review. *Mol Pharm* 3: 198–211.
- Ghibellini G, Vasist LS, Leslie EM, Heizer WD, Kowalsky RJ, Calvo BF, et al. (2007). In Vitro–In Vivo Correlation of Hepatobiliary Drug Clearance in Humans (2007). *Clin Pharmacol Ther* 81: 406–413.
- Gilbert MR, Kuhn J, Lamborn KR, Lieberman F, Wen PY, Mehta M, et al. (2012). cilengitide in patients with recurrent glioblastoma: the results of NABTC 03-02, a phase II trial with measures of treatment delivery. *J Neurooncol* 106: 147–153.
- Kurozumi K, Ichikawa T, Onishi M, Fujii K, Date I (2012). Cilengitide treatment for malignant glioma: Current status and future direction. *Neurol Med Chir (Tokyo)* 52: 539–547.
- Letschert K, Faulstich H, Keller D, Keppler D (2006). Molecular characterization and inhibition of  $\alpha$ -amanitin uptake into human hepatocytes. *Toxicol Sci* 91: 140–149.
- MacDonald TJ, Shimada H, Cheresch DA, Laug WE (1999). Antagonist to  $(\alpha v)$  integrins inhibits growth of orthotopically but not heterotopically transplanted brain tumors. *Proc Amer Assoc Cancer Res* 40: 4096.
- MacDonald TJ, Taga T, Shimada H, Tabrizi P, Zlokovic BV, Cheresch DA, et al. (2001). Preferential susceptibility of brain tumors to the antiangiogenic effects of an  $\alpha v$  integrin antagonist. *Neurosurgery* 48: 151–157.
- Mas-Moruno C, Rechenmacher F, Kessler H (2010). Cilengitide: the first anti-angiogenic small molecule drug candidate design, synthesis and clinical evaluation. *Anticancer Agents Med Chem* 10: 753–768.
- Maurer GD, Tritschler I, Adams B, Tabatabai G, Wick W, Stupp R, et al. (2009). Cilengitide modulates attachment and viability of human glioma cells, but not sensitivity to irradiation or temozolomide in vitro. *Neuro Oncol* 11: 747.
- Mitjans F, Meyer T, Fittschen C, Goodman S, Jonczyk A, Marshall JF, et al. (2000). In vivo therapy of malignant melanoma by means of antagonists of  $\alpha v$  integrins. *Int J Cancer* 87: 716–723.
- Miyamoto S, Teramoto H, Gutkind JS, Yamada K (1996). Integrins can collaborate with growth factors for phosphorylation of receptor tyrosine kinases and MAP kinase activation: roles of integrin aggregation and occupancy of receptors. *J Cell Biol* 135: 1633–1642.
- Moehler TM, Neben K, Goldschmidt H (2001). Angiogenesis in hematologic malignancies. *Ann Hematol* 80: 695–705.

O'Donnell PH, Undevia SD, Stadler WM, Karrison TM, Nicholas MK, Janisch L (2010a). A phase I study of continuous infusion cilengitide in patients with solid tumors. *Invest New Drugs* 30: 604–610.

Raguse JD, Gath HJ, Bier J, Riess H, Oettle H (2004). Cilengitide (EMD 121974) arrests the growth of a heavily pretreated highly vascularised head and neck tumour. *Oral Oncol* 40: 228–230.

Soffiatti R, Trevisan E, Ruda R (2014). What have we learned from trials on antiangiogenic agents in glioblastoma? *Expert Rev Neurother* 14: 1–3.

Stupp R, Hegi ME, Neyns B, Goldbrunner R, Schlegel U, Clement PM, *et al.* (2010). Phase I/IIa study of cilengitide and temozolomide with concomitant radiotherapy followed by cilengitide and temozolomide maintenance therapy in patients with newly diagnosed glioblastoma. *J Clin Oncol* 28: 2712–2718.

Tentori L, Dorio AS, Muzi A, Lacial PM, Ruffini F, Navarra P, *et al.* (2008). The integrin antagonist cilengitide increases the antitumor activity of temozolomide against malignant melanoma. *Oncol Rep* 19: 1039–1043.

Wallace RJ (1997). Peptidase Activity of Human Colonic Bacteria. *Anaerobe* 3: 251–257.

Wu CY, Benet LZ (2005). Predicting drug disposition via application of BCS: transport/absorption/elimination interplay

and development of a biopharmaceutics drug disposition classification system. *Pharm Sci* 22: 11–23.

Yamada S, Bu XY, Khankaldyyan V, Gonzales-Gomez I, McComb JG, Laug WE (2006). Effect of the angiogenesis inhibitor cilengitide (EMD 121974) on glioblastoma growth in nude mice. *Neurosurgery* 59: 1304–1312.

## Supporting Information

Additional Supporting Information may be found in the online version of this article:

**Figure S1.** NADPH-dependent metabolism of 14C-cilengitide (EMD121974) by male mouse liver microsomes.

**Figure S2.** NADPH-dependent metabolism of 14C-cilengitide (EMD121974) by male monkey liver microsomes.

**Figure S3.** NADPH-dependent metabolism of 14C-cilengitide (EMD121974) by a pool of human liver microsomes.

**Figure S4.** Metabolism of 14C-cilengitide in rat hepatocytes.

**Figure S5.** Metabolism of 14C-cilengitide in human hepatocytes.

**Table S1.** Apparent permeability of cilengitide (MSC 1097999C) in Caco-2 cells.

**Table S2.** Radio-HPLC condition.